Magnetic anisotropy and field switching in cobalt ferrite thin films deposited by pulsed laser ablation

T. Dhakal,[a),b)] D. Mukherjee,[b)] R. Hyde, P. Mukherjee, M. H. Phan, H. Srikanth, and S. Witanachchi[a)]

Department of Physics and Center for Integrated Functional Materials (CIFM), University of South Florida, Tampa, Florida 33620, USA

(Received 9 October 2009; accepted 26 January 2010; published online 11 March 2010)

We report the observation of contrasting magnetic behavior in cobalt ferrite (CFO) thin films deposited on single crystalline magnesium oxide (MgO) and strontium titanate (STO). Epitaxial films on MgO (100) with a lattice mismatch of 0.35% showed out-of-plane anisotropy whereas the films on STO (100) with a lattice mismatch of 7.4% displayed in-plane anisotropy. Stress anisotropy calculated from angle-dependent x-ray diffraction analysis confirmed that the change in anisotropy originates from the lattice mismatch. An additional low-field switching characteristic is observed in the M-H loops of the CFO films, which became prominent with lowering temperature as also evidenced from the rf transverse susceptibility measurements. The obtained results revealed that the low field switching is associated with the film-substrate interface. © *2010 American Institute of Physics*. [doi:10.1063/1.3327424]

I. INTRODUCTION

Cobalt ferrite ($CoFe_2O_4$) (CFO) is a hard magnetic material with high degree of magnetic anisotropy and magnetostriction. The unique magnetic properties of this material can be understood from its electronic and structural configurations. The divalent cobalt and trivalent iron cations are located on the octahedral and tetrahedral sites, respectively, as in an inverse spinel structure. In a normal spinel structure (AB_2O_4), the A^{2+} cations occupy the tetrahedral sites whereas the B^{3+} cations occupy the octahedral sites. However, in an inverse spinel structure, half of the octahedral coordination sites are occupied by A^{2+} cations and the remaining half as well as all the tetrahedral coordination sites are occupied by the B^{3+} cations. A unit cell of CFO which is a face-centered cubic (fcc) structure with lattice parameter (a_o) of 8.39 Å, consists of eight formula units.[1] The eight Fe^{3+} ions in tetrahedral sites are aligned antiferromagnetically with respect to the remaining eight Fe^{3+} ions via superexchange interactions mediated by oxygen ions. Thus the uncompensated Co^{2+} ions which have three unpaired electrons in their *d*-orbitals would give a theoretical saturated magnetization value of 3 μ_B per formula unit or in other words per Co site. However, the experimental value of the saturated magnetization in CFO is found to be around 4 μ_B. This discrepancy between the theoretical and experimental values could be attributed to two factors.[1] First, the calculation was done by neglecting the contribution from the orbital motion of electrons. Second, the Fe^{3+} moments were assumed to be aligned perfectly anti-parallel, but in reality they may be canted. In addition, the distribution of different ions may not be as perfect as assumed.

The first order magnetocrystalline anisotropy (K_1) energy constant for CFO has been reported to be of the order of 10^6 erg/cm^3, which is one of the highest for ferrites.[2] The anisotropy direction changes depending on the growth conditions,[3,4] the choice of substrate, and whether the film is grown under compression or tension.[5,6] The large magnetocrystalline anisotropy and the tendency of the CFO to grow with the easy axis perpendicular to the substrate, if grown under tension, makes this an attractive material for applications in magneto-optic recording.[1] This is because, if the magnetic easy axis is perpendicular to the substrate, a beam of laser light pointed directly into the film will then interact easily via Faraday rotation. This material also has a very high magnetostriction coefficient (λ). Reference 2 reported the values of λ_{100} for CFOs in the range between -200×10^6 to -590×10^6. The high magnetostriction in CFO, coupled with its large magnetocrystalline anisotropy, make it a suitable material for integration into multilayered or composite forms of multiferroic structures. Epitaxial composites[7,8] of CFO and lead zirconate titanate ($PbZr_xTi_{1-x}O_3$) (PZT) have been reported to exhibit multiferroicity. Strong magnetoelastic coupling is observed in the vertically self-assembled nanostructure composite of $BaTiO_3-CoFe_2O_4$ at the ferroelectric Curie temperature.[9] Similar strain mediated magnetoelastic coupling between columnar epitaxial $BiFeO_3$ and $CoFe_2O_4$ nanocomposites have induced magnetic reversal.[10]

The resistivity of CFO is relatively high ($\sim10^7$ Ω cm).[1] In addition ferrites are reported to have large permeability at high frequency ($\sim$1000 MHz).[1,3] Since the square of the depth of penetration of the applied magnetic field is directly proportional to the frequency and the permeability, and inversely proportional to the resistivity,[1] CFO can find applications in microwave devices. Because of the good insulating properties and high Curie temperature, an experimental evidence of room temperature spin filtering in magnetic tunnel junctions (MTJ) containing $CoFe_2O_4$ is observed by

[a)]Electronic addresses: tdhakal@cas.usf.edu and switanac@cas.usf.edu.
[b)]These authors contributed equally.

Ramos[11] and the group. Across such MTJs, they observed tunneling magnetoresistance values of −18% and −3% at 2 and 290 K, respectively.

As discussed above, CFO thin films have a great potential for use in technological applications varying from magnetic recording to microwave devices. Exploitation of the study of magnetic behavior of CFOs is thus essential to accomplish the aforementioned possibilities. For this purpose, our work will focus on tuning the magnetic anisotropy in CFO thin films with lattice mismatch strain and explain the anomalies observed thereafter. Single crystalline substrates with varying lattice parameters are used to introduce varying strain at the film-substrate interface and the magnetic anisotropy in the produced films is studied. A change in magnetic anisotropy is observed as the thin films of CFO were grown from one substrate to another. In addition, a low field switching is observed for the first time in intrinsic CFO thin films. Such switching is observed in bilayers of CFO and other magnetic materials.[12,13] Suzuki *et al.*[12] show that the switching is due to the strong exchange coupling between CFO thin film and magnetically soft $(Mn,Zn)Fe_2O_4$ at room temperature. They showed an inverse linear dependence of exchange field on $(Mn,Zn)Fe_2O_4$ thickness, which is an evidence for the interfacial nature of the interaction. Ramos and co-workers[13] demonstrated that the switching behavior in the epitaxial bilayer of $CoFe_2O_4$ and Fe_3O_4 is due to the magnetic interaction at the bilayer interface, but not from the intrinsic properties of the either of the individual layers. We observed the low field switching behavior in the intrinsic CFO monolayer film and have shown quantitatively that it arises from the interface between the film and the substrate.

II. EXPERIMENT

We have grown epitaxial CFO on lattice matched substrates such as magnesium oxide (MgO) and strontium titanate (STO) in order to investigate their influence on magnetic anisotropy. Films of thickness around 200 nm were deposited on MgO (100) and STO (100) substrates using pulsed laser ablation. An excimer laser of wavelength 248 nm was used to ablate a compressed powder target of CFO. The chamber was kept at 10 mTorr pressure of oxygen during the growth while heating the substrate to 450 °C. The repetition rate of the laser pulse was kept at 10 Hz and the fluence at the target surface was 2 J/cm^2. The distance between the substrate and the target was 6 cm. Under these growth conditions, the rate of growth was measured to be around 0.1 Å/pulse. The film crystallinity and orientation were assessed by conventional θ-2θ x-ray diffraction (XRD) method, Φ-scan and rocking curve techniques. The stress on the film was measured using the standard $\sin^2\psi$ technique. In-plane lattice parameters were obtained from the asymmetric XRD scans around some particular planes. The magnetization of these films was measured with a physical property measurement system (PPMS) from quantum design. A sensitive rf transverse susceptibility (TS) method based on a self-resonant tunnel diode oscillator (TDO) (Ref. 14) integrated into the PPMS, was also employed to study the low field switching and anisotropy characteristics of the CFO thin films.

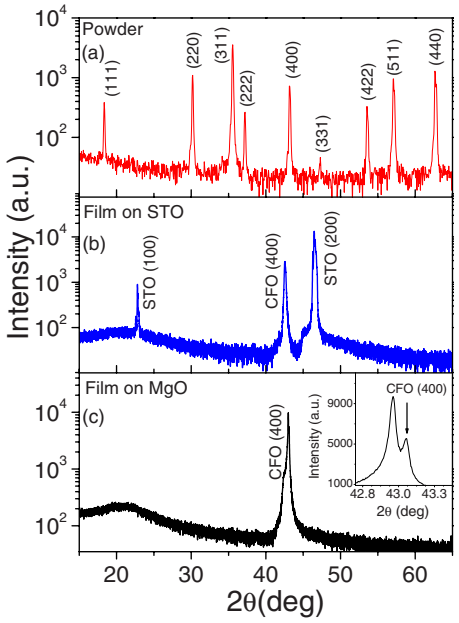

FIG. 1. (Color online) (a) XRD peaks of powder target of CFO. (b) XRD peak of epitaxial 200 nm thick film of CFO grown on STO (100) substrate. The peak from CFO (400) is shifted toward the left due to large lattice mismatch with substrate. The left and right peaks are from the substrate. (c) XRD peak of epitaxial 200 nm thick film of CFO grown on MgO (100) substrate. The (400) peak of CFO appears overlapped with the (200) peak of MgO. The inset is a close up view, which clearly shows both MgO (200) (left) and CFO (400) (right) peaks.

III. RESULTS AND DISCUSSIONS

A. Crystallinity and stoichiometry

Figure 1 shows the XRD peaks for the powder target and the films grown on MgO and STO substrates. The powder target showed all the characteristic peaks [Fig. 1(a)] of CFO.[15,16] The peaks that appear match with CFO fcc lattice with space group Fd-3m (227). The films grown on MgO (100) and STO (100) show epitaxial growth [Figs. 1(b) and 1(c)]. The θ-2θ peaks show only (400) peak of CFO and no trace of any impurity peak even in the logarithmic scale. A close up view shows both CFO (400) and MgO (200) peaks side by side as shown in the inset of Fig. 1(c). Figures 2(b) and 2(e) show the (400) rocking curves of the lattice-matched CFO grown on STO and MgO, respectively. The full width at half maximum (FWHM) for the film grown on MgO is 0.076°, which confirms an excellent crystallographic texture along (100). Since (200) of MgO and (400) of CFO are very close to each other, Φ-scan measurements were conducted using Bragg's reflection from (311) plane of CFO [Fig. 2(d)]. The peaks of the Φ spectra occur at intervals of 90° confirming the cubic symmetry and in-plane epitaxial growth. Because of larger lattice mismatch in the case of the film grown on STO substrate, (400) peak of CFO is shifted significantly as shown in Fig. 1(b). In addition, FWHM is also large (0.915°) in the case of the film grown on STO substrate [Fig. 2(b)]. Φ-scan curves from (311) reflection of CFO film grown on STO substrate as shown in Fig. 2(a) demonstrate excellent in-plane epitaxy. Because of the shift in the CFO peak on the film grown on STO, the film lattice could be tetragonally distorted. In-plane lattice parameters

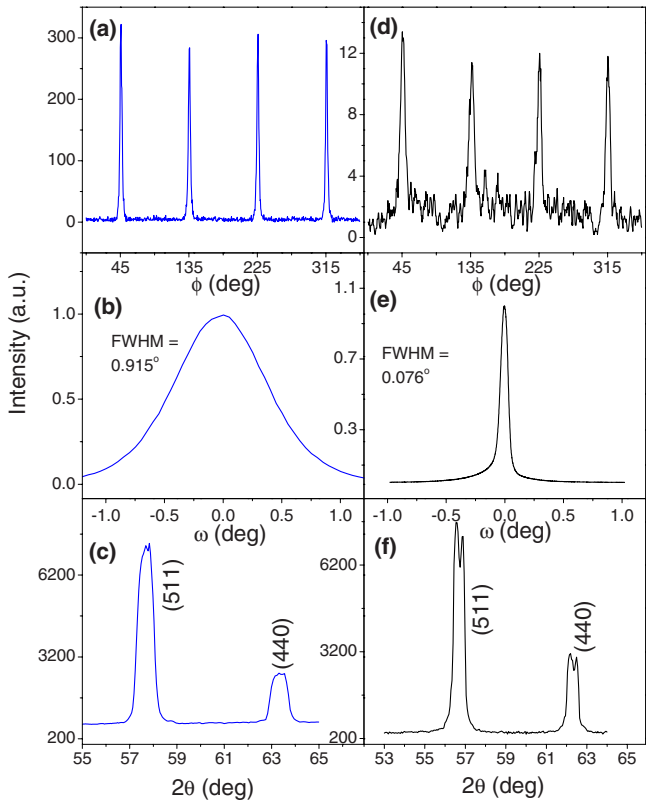

FIG. 2. (Color online) Left column of graphs represent the film grown on STO and the right column represents films grown on MgO. (a) and (d) Φ scan spectra from (311) reflection. (b) and (e) Rocking curve of CFO (400) peaks. (c) and (f) Asymmetric scans of the (511) and (440) textures of the CFO films. The in-plane lattice parameters are obtained from these scans.

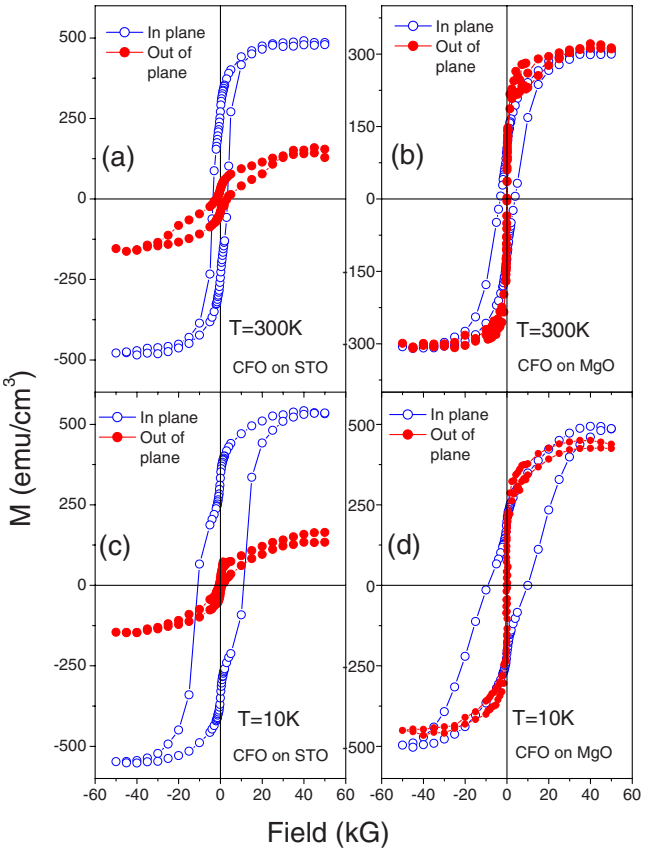

FIG. 3. (Color online) (a) and (c) M-H loops measured at 300 and 10 K, respectively, of the 200 nm thin film grown on STO (100) for in-plane and out-of-plane configuration. (b) and (d) M-H loops measured at 300 and 10 K, respectively, of the 200 nm thin film grown on MgO (100) for in-plane and out-of-plane configuration.

were obtained from the asymmetric scan of the two CFO planes, viz., (511) and (440) [Figs. 2(c) and 2(f)]. The value of the in-plane lattice parameter given in Table I is the average of the values obtained from the reflections off of these two planes. The difference between the out-of-plane lattice parameter ($a_\perp$=8.486 Å) and the in-plane lattice parameter ($a_\parallel$=8.297 Å) confirms the tetragonal distortion in the film grown on STO. In the case of the film grown on MgO, in-plane and out-of-plane lattice parameter differ by only 0.15%. Values of in-plane strain presented in Table I are calculated by using the formula $(a_\parallel - a_o)/a_o$. To confirm the stoichiometry, energy dispersive spectroscopy (EDS) was used. In each of the thin films of $CoFe_2O_4$ used, it was found that the Fe:Co ratio was very close to 2 (Table I). This confirms the single crystalline stoichiometric growth of CFO thin films.

B. Magnetization measurements

Magnetic measurements were conducted for in-plane and out-of-plane configurations of the films in magnetic fields up to 50 kOe. Figure 3 shows the M-H loops measured at 300 and 10 K for the epitaxial thin films of the same thickness (200 nm). The hysteresis graphs in Fig. 3 were obtained after subtracting the diamagnetic contribution from the substrates. The saturation magnetization (M_s) value of the film grown on STO at 300 K is around 490 emu/cm^3 which corresponds to 3.9 μ_B per Co-site. This value is around 2.6 μ_B per Co-site in case of the film grown on MgO. However, at low temperature (10 K), the saturation magnetization is closer to the bulk value of the CFO.[1] One of the reasons could be that the Curie temperature of the films grown on MgO might have decreased. It can be observed

TABLE I. Co to Fe ratio obtained by energy dispersive x-ray analysis (EDS), in-plane and out-of-plane lattice parameters obtained from XRD peaks, and the strain calculated using in-plane lattice parameters.

CFO film on	Co/Fe ratio	$a_\perp$ (Å)	$a_\parallel$ (Å)	In-plane strain	Stress (dyn/cm^3)	Anisotropy (K_a) (erg/cm^3)
MgO	2.040	8.388	8.401	0.0013	-12.19×10^9 [a]	10.79×10^6
STO	2.014	8.486	8.297	−0.011	-16.50×10^9	14.60×10^6

[a]In case of the film grown on MgO, $\sin^2\psi$ technique is used to calculate the stress. Anisotropy is calculated by using the stress.

that the easy axis of magnetization of the films grown on MgO is out of the plane of the film along the [100] direction, whereas the films grown on STO have the easy axis of magnetization along the plane of the film. We would like to point out that the easy axis in case of the film grown on MgO is not well defined. Although, the saturation field is smaller for the out-of-plane magnetization, the coercivity is small, atypical for an easy axis. However, the difference in magnetic anisotropy for these two films could have arisen from the fact that the CFO films (lattice constant=8.39 Å) grow with tensile strain on MgO (2×lattice parameter=8.42 Å) substrate and undergo compression when grown on STO (2×lattice parameter=7.81 Å). In particular, the stress present due to the mismatch between the film and the substrate may have played a significant role in the observed anisotropy.

To address this, we have calculated the uniaxial anisotropy by using the difference between the in-plane and out-of-plane magnetization obtained from Fig. 3. The uniaxial magnetic anisotropy is given by[17]

$$K_u = \int_0^{M_s} (H_{\text{eff}}^{\text{out}} - H_{\text{eff}}^{\text{in}}) dM, \tag{1}$$

where $H_{\text{eff}}=H_{\text{ex}}-NM$, N=demagnetization factor, M=magnetization, H_{ex} the external field applied, and M_s is the saturation magnetization. The superscripts *out* and *in* correspond to the out-of-plane and in-plane orientation of the films with respect to the applied magnetic field. For the case of a thin film with uniform magnetization in all x, y, and z direction, Eq. (1) reduces to

$$K_u = H_{\text{ex}}^{\text{out}} M_s^{\text{out}} - H_{\text{ex}}^{\text{in}} M_s^{\text{in}} - \frac{1}{2}(M_s^{\text{out}})^2 \tag{2}$$

The uniaxial magnetic anisotropy calculated for the film grown on MgO substrate is $K_u=9.13\pm0.34\times10^6$ erg/cm^3. This value of K_u is threefold larger than the intrinsic magnetocrystalline anisotropy of bulk CFO (3×10^6 erg/cm^3).[2,3] This indicates that the large anisotropy seen in the film grown on MgO likely arises from the presence of large stress due to the mismatch between the film and the substrate.

For the case of the films grown on STO (100), the out-of-plane magnetization is not saturated up to an applied field of 50 kOe (see Fig. 3). Therefore, it is not precise to use Eq. (2) to estimate the magnetic anisotropy for this film. Alternatively, we have estimated the magnetic anisotropy of this film by using the difference between the lattice parameter of bulk (8.39 Å) CFO and the corresponding thin film (8.297 Å). This large change in the thin film value is caused by the large mismatch between the lattice parameter of CFO and the STO substrate ($2\times3.905=7.81$ Å). The strain (ε) due to the difference between the bulk and in-plane film lattice constant is -0.011. Thus the stress $\sigma=Y\,\varepsilon$ (Young's modulus[2] $Y_{100}=1.5\times10^{12}$ dyne/cm^2) is -16.50×10^9 dyne/cm^2. Magnetoelastic stress anisotropy constant can be estimated by $K_a=(3/2)\,\lambda_{100}\,\sigma$, where λ_{100} for CFO (Refs. 2 and 3) is -590×10^{-6}. K_a calculated this way is 14.6×10^6 erg/cm^3. This value is larger compared to that obtained for the film grown on MgO (100). This is consistent with the fact that stress is larger for the film grown on STO than for the film grown on MgO. It is the presence of larger stress in the film grown on STO that causes a larger shift in the (400) Bragg reflection compared to the bulk [Figs. 1(a) and 1(b)]. The anisotropy field (H_a) of the film grown on STO is estimated to be about 59.6 kOe, using the expression $H_a=2K_a/M_s$.

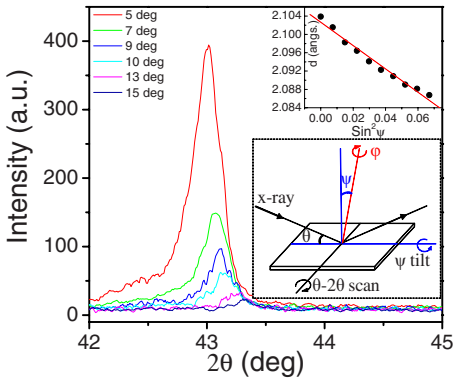

FIG. 4. (Color online) θ-2θ scan about $2\theta=43.006°$ by varying the ψ angle from 0° to 15° keeping the φ at 0° on the CFO films on MgO (100) substrate. The legend shows the values of ψ. The upper inset shows the plot of d vs $\sin^2\psi$ and a linear fit to the data points. Schematic for $\sin^2\psi$ technique is shown in the lower inset.

C. Stress measurement ($\sin^2\psi$ technique)

To provide further insights into the importance of stress in the observed anisotropy in the CFO thin films, we have used the $\sin^2\psi$ technique (the direct stress measurement technique) to evaluate the stress and hence the anisotropy of the films grown on MgO. Since the in-plane lattice parameter ($a_{\parallel}=8.401$ Å) is very close to the bulk lattice parameter ($a_o=8.390$ Å) for the film grown in MgO, stress in this case is measured using this method. The $\sin^2\psi$ technique is a standard nondestructive technique to measure residual stress in a material. In this technique, a textured film is scanned in the vicinity of the Bragg reflection (2θ). A shift in the Bragg reflection (2θ) is observed if a strained film is tilted by an angle (ψ). The schematic is shown in the lower inset of Fig. 4. The shift in 2θ is used to calculate the new value of interplanar spacing (d). It has been found that d is linearly varied as a function of $\sin^2\psi$ as shown below[18]

$$d_\psi = \left(\frac{1+\nu}{Y}\right) d_0 \sigma \sin^2\psi - \frac{\nu}{Y}(\sigma_{11}+\sigma_{22}) d_0 + d_0. \tag{3}$$

The slope of d_ψ and $\sin^2\psi$ gives the value of the stress σ if the Poisson's ratio (ν) and the Young's modulus (Y) of the particular material are known. d_0 is the interplanar distance corresponding to the unstrained cubic lattice. It should be noted here that above relation is modified for $\varphi=0$.

Figure 4 shows the 2θ scans of CFO–MgO film for various ψ tilts. The values of d were calculated using the shift in the Bragg reflection for different tilt (ψ) angles. The different values of d are plotted as a function of $\sin^2\psi$ (Upper inset of Fig. 4). A fairly linear curve was observed indicating that the residual stress within the area under scan was nearly homogeneous. The slope of the curve obtained provides a qualitative measurement of the residual stress in the thin films. By

using the slope of the fit and equating that to the coefficient of $\sin^2\psi$ term in Eq. (3) we have calculated the stress (σ) for CFO–MgO to be $\sigma=-12.19\times10^9$ dyne/cm^2. Due to the proximity of the substrate and the film peak, a background due to MgO substrate was subtracted from the slope. The values Y, ν, and d_0 used were as follows for CFO: $Y=1.5\times10^{12}$ dyne/cm^2, $\nu=0.26$[19] and $d_0=2.0979$ Å. The stress anisotropy (K_a) is obtained from $K_a=(3/2)\,\lambda_{100}\,\sigma$, where λ_{100} for CFO is -590×10^{-6} and $\sigma=-12.19\times10^9$ dyne/cm^2, to be 10.79×10^6 erg/cm^3. The value of Y and λ are specific for [100] direction and thus are good estimates for our epitaxial films. A possible error in the calculation could be due to the bulk Poisson's ratio (ν) used. However, by changing ν by 25%, the value of anisotropy (K_a) changes by only around 5%. The value of the anisotropy thus obtained is very close to that calculated from the M-H data using Eq. (2) ($K_u=9.13\times10^6$ erg/cm^3). The consistency of these two independent methods clearly indicates that stress plays a dominant role in the observed anisotropy in the CFO thin films grown on lattice mismatched substrates. The anisotropy field (H_a) of the film grown on MgO is determined to be about 66.8 kOe, whereas that for the film grown on STO is 59.6 kOe.

D. Probing magnetic switching using rf TS

While the low field switching feature is clearly observed in the M-H loops, it is difficult to determine precisely magnetic switching field and particularly its dependence on measuring temperature. In this work, we have used a very sensitive and precise rf TS technique developed by Srikanth *et al.*[14] to probe magnetic switching and its temperature dependence in both the film grown on STO and the film grown on MgO. The rf TS, which is based on a sensitive, self-resonant TDO, has been validated over the years to be an excellent technique for probing effective magnetic anisotropy and switching in a wide range of magnetic materials ranging from thin films,[20] nanoparticles[21] to single crystals.[22] In TS experiments, a small perturbing ac or rf field (<10 Oe) is applied to the sample in addition to the swept dc magnetic field. Since the sample is placed in an inductive rf coil that is part of a self-resonant circuit, the shift in the resonant frequency with varying dc magnetic field and/or temperature give a direct measure of the change in inductance and hence the sample susceptibility. The change in TS with dc magnetic field has been expressed by

$$\left(\frac{\Delta\chi_T}{\chi_T}\right)\% = \left[\frac{\chi(H)-\chi(H_{\max})}{\chi(H_{\max})}\right]\times 100\%, \quad (4)$$

where $H_{\max}$ is the maximum applied dc magnetic field.

Theoretically, the TS spectrum in a unipolar field scan from positive to negative saturation should consist of three singularities of which two occur at the anisotropy fields ($\pm H_k$) and one at the switching field ($\pm H_s$).[23,24] However, it has been experimentally shown that depending upon the magnetic nature of the sample and the orientation in which the sample is introduced in the inductive coil, either anisotropy peaks or switching peaks could be prominently observed.

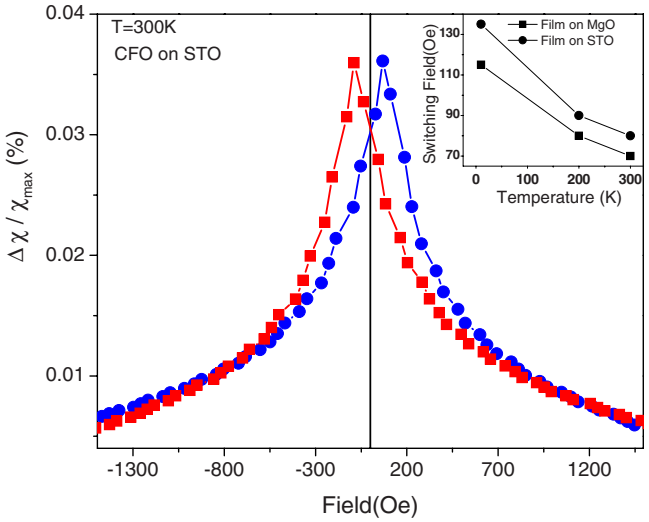

FIG. 5. (Color online) TDO measurement of CFO films on STO at 300 K with the film plane perpendicular to the dc field. The line with solid square represent the field sweep from positive to negative, where as the solid circles represent the field sweep from negative to positive.

In the present study, rf TS measurements were conducted at different temperatures ($T=300$, 200, and 10 K) for the CFO films grown on both MgO and STO. The maximum dc field applied was 5 kOe. The results are displayed in Fig. 5 and its inset. It can be clearly seen from this figure that the TS curves show only switching peak, but no anisotropy peaks are detected. The absence of anisotropy peaks can be understood due to the fact that the anisotropy fields of the films investigated were beyond the maximum applied dc magnetic field. However, it was possible to detect the low field switching present in the CFO films. The change of TS peak position with temperature (see inset of Fig. 5) clearly reveals that for the CFO films investigated, the switching field increases as the temperature is decreased. For the film grown on MgO, the switching fields at 300, 200, and 10 K were ±70, ±80, and ±115 Oe, respectively. In case of the film grown on STO, the switching fields obtained for 300, 200, and 10 K were ±80, ±90, and ±135 Oe, respectively. The larger values of switching field for the case of the film grown on STO may be reconciled with the fact that the lattice mismatch and thus the stress is larger in this sample. The stress due to lattice mismatch would be more significant at the interface. This indicates that the origin of the steps seen in the M-H loops of the CFO films is associated with the stress at the interface between the substrate and the film.

IV. CONCLUSIONS

We showed that stress is a dominant factor in the observed anisotropy in single crystalline thin films of CFO. The film with larger strain (on STO substrate) showed larger stress anisotropy. Films grown on STO experienced compression and showed in-plane anisotropy. On the other hand, films grown on MgO with tensile strain exhibited easy out-of-plane switching, which will have a good application in magneto optical recording devices. An additional step like feature at low field is attributed to the soft magnetic switching of the domains at the film-substrate interface. However,

further investigation is needed to find the microscopic mechanism of the magnetic switching at the interface.

ACKNOWLEDGMENTS

This work was supported in part by the National Science Foundation under the Grant Nos. DMI-0217939 and DMI-0078917 and by the Department of Defense under the Grant No. W81XWH-07-1-0708. H.S. also acknowledges support from DOE through Grant No. DE-FG02-06ER46275. We would like to thank Prof. Amlan Biswas and Marienette Morales for helping us with magnetic measurements.

[1]A. Goldman, *Modern Ferrite Technology*, 2nd ed. (Springer, New York, 2006).
[2]R. M. Bozorth, E. F. Tilden, and A. J. Williums, Phys. Rev. **99**, 1788 (1955).
[3]P. D. Thang, G. Rijnders, and D. H. A. Blank, J. Magn. Magn. Mater. **310**, 2621 (2007).
[4]P. C. Dorsey, P. Lubitz, D. B. Chrisey, and J. S. Horwitz, J. Appl. Phys. **79**, 6338 (1996).
[5]Y. Suzuki, G. Hu, R. B. van Dover, and R. J. Cava, J. Magn. Magn. Mater. **191**, 1 (1999).
[6]G. Hu, J. H. Choi, C. B. Eom, V. G. Harris, and Y. Suzuki, Phys. Rev. B **62**, R779 (2000).
[7]N. Ortega, P. Bhattacharya, R. S. Katiyar, P. Dutta, A. Manivannan, M. S. Seehra, I. Takeuchi, and S. B. Majumder, J. Appl. Phys. **100**, 126105 (2006).
[8]J.-P. Zhou, Z.-C. Qiu, and P. Liu, Mater. Res. Bull. **43**, 3514 (2008).
[9]H. Zheng, J. Wang, S. E. Lofland, Z. Ma, L. Mohaddes-Ardabili, T. Zhao, L. Salamanca-Riba, S. R. Shinde, S. B. Ogale, F. Bai, D. Viehland, Y. Jia, D. G. Schlom, M. Wuttig, A. Roytburd, and R. Ramesh, Science **303**, 661 (2004).
[10]F. Zavaliche, H. Zheng, L. Mohaddes-Ardabili, S. Y. Yang, Q. Zhan, P. Shafer, E. Reilly, R. Chopdekar, Y. Jia, P. Wright, D. G. Schlom, Y. Suzuki, and R. Ramesh, Nano Lett. **5**, 1793 (2005).
[11]A. V. Ramos, M.-J. Guittet, J.-B. Moussy, R. Mattana, C. Deranlot, F. Petroff, and C. Gatel, Appl. Phys. Lett. **91**, 122107 (2007).
[12]Y. Suzuki, R. B. van Dover, E. M. Gyorgy, J. M. Phillips, and R. J. Felder, Phys. Rev. B **53**, 14016 (1996).
[13]A. V. Ramos, J.-B. Moussy, M.-J. Guittet, M. Gautier-Soyer, C. Gatel, P. Bayle-Guillemaud, B. Warot-Fonrose, and E. Snoeck, Phys. Rev. B **75**, 224421 (2007).
[14]H. Srikanth, J. Wiggins, and H. Rees, Rev. Sci. Instrum. **70**, 3097 (1999).
[15]R. Sayed Hassan, N. Viart, C. Ulhaq-Bouillet, J. L. Loison, G. Versini, J. P. Vola, O. Crégut, G. Pourroy, D. Muller, and D. Chateigner, Thin Solid Films **515**, 2943 (2007).
[16]H. E. Swanson, H. F. McMurdie, M. C. Morris, E. H. Evans, B. Paretzkin, J. H. DeGroot, and S. J. Carmel NBS Monogr. **25**, 22 (1971).
[17]J. H. Yin, J. Ding, B. H. Liu, J. B. Yi, X. S. Miao, and J. S. Chen, J. Appl. Phys. **101**, 09K509 (2007).
[18]I. C. Noyan and J. B. Cohen, *Residual Stress* (Springer-Verlag, Berlin, 1987).
[19]S. R. Murthy, Cryst. Res. Technol. **25**, 461 (1990).
[20]N. A. Frey, S. Srinath, H. Srikanth, M. Varela, S. Pennycook, G. X. Miao, and A. Gupta, Phys. Rev. B **74**, 024420 (2006).
[21]P. Poddar, J. L. Wilson, H. Srikanth, D. F. Farrell, and S. A. Majetich, Phys. Rev. B **68**, 214409 (2003).
[22]G. T. Woods, P. Poddar, H. Srikanth, and Ya. M. Mukovskii, J. Appl. Phys. **97**, 10C104 (2005).
[23]A. Aharoni, E. H. Frei, S. Shtrikman, and D. Treves Bull. Res. Counc. Isr., Sect. F **6A**, 215 (1957).
[24]L. Spinu, H. Srikanth, A. Gupta, X. W. Li, and G. Xiao, Phys. Rev. B **62**, 8931 (2000).